Article

Integrative Transcriptomic and Metabolomic Analysis of Muscle and Liver Reveals Key Molecular Pathways Influencing Growth Traits in Zhedong White Geese

Kai Shi [1], Xiao Zhou [1], Jiuli Dai [1], Yuefeng Gao [2], Linna Gao [3,4], Yangyang Shen [3,5,*] and Shufang Chen [1,*]

[1]   Ningbo Academy of Agricultural Sciences, Institute of Livestock and Poultry Research, Ningbo 315040, China;
     shikai2024@126.com (K.S.)
[2]   College of Applied Engineering, Henan University of Science and Technology, Sanmenxia 472000, China;
     nexhyf@hotmail.com
[3]   Institute of Animal Science, Jiangsu Academy of Agricultural Sciences, Nanjing 210014, China
[4]   School of Life Sciences and Food Engineering, Hebei University of Engineering, Handan 056038, China
[5]   Key Laboratory of Crop and Animal Integrated Farming, Ministry of Agriculture and Rural Affairs,
     Nanjing 210014, China
[*]   Correspondence: sy2azy@163.com (Y.S.); 13606780161@163.com (S.C.)

Simple Summary: This study explored the growth mechanisms of geese by analyzing transcriptomic and metabolomic differences between high-weight (HW) and low-weight (LW) Zhedong White geese. The HW geese exhibited significantly higher body weight and average daily gain than LW geese, with no significant difference in the yields of certain organs. In the breast muscle, 19 differentially expressed genes (DEGs) related to pathways like PPAR signaling and fatty acid biosynthesis were found, along with 59 differential accumulation metabolites (DAMs) affecting glutathione and vitamin B6 metabolism. In the liver, 106 DEGs and 202 DAMs were identified, influencing various metabolic pathways. Correlation analysis revealed links between specific gene expressions and metabolite levels. These findings enhance the understanding of goose growth and provide molecular markers for breeding.

Abstract: Geese (*Anser cygnoides*) are popular worldwide with consumers for their unique meat quality, egg production, foie gras, and goose down; however, the key genes that influence geese growth remain elusive. To explore the mechanism of geese growth, a total of 500 Zhedong White geese were raised; four high-weight (HW) and four low-weight (LW) male geese were selected to collect carcass traits and for further transcriptomic and metabolomic analysis. The body weight and average daily gain of HW geese were significantly higher than those of the LW geese (p-value < 0.05), and the yields of the liver, gizzard, glandular stomach, and pancreas showed no significant difference between the HW and the LW group (p-value > 0.05). Compared with the LW geese, 19 differentially expressed genes (DEGs) (i.e., *COL11A2*, *COL22A1*, and *TF*) were detected in the breast muscle from the HW geese, which were involved in the PPAR signaling pathway, adipocytokine signaling pathway, fatty acid biosynthesis, and ferroptosis. A total of 59 differential accumulation metabolites (DAMs), which influence the pathways of glutathione metabolism and vitamin B6 metabolism, were detected in the breast muscle between the HW and LW geese. In the liver, 106 DEGs (i.e., *THSD4*, *CREB3L3*, and *CNST*) and 202 DAMs were found in the livers of the HW and LW groups, respectively. DEGs regulated the pathways of the TGF-beta signaling pathway, pyruvate metabolism, and adipocytokine signaling pathway; DAMs were involved in pyrimidine metabolism, nitrogen metabolism, and phenylalanine metabolism. Correlation analysis between the top DEGs and DAMs revealed that in the breast muscle, the expression levels of *COL11A2* and *COL22A1* were positively correlated with the content of S-(2-Hydroxy-3-buten-1-yl)glutathione. In the liver, the expression

of *THSD4* was positively correlated with the content of 2-Hydroxyhexadecanoic acid. In addition, one DEG (*LOC106049048*) and four DAMs (mogrol, brassidic acid, flabelline, and L-Leucyl-L-alanine) were shared in the breast muscle and liver. These important results contribute to improving the knowledge of goose growth and exploring the effective molecular markers that could be adopted for Zhedong White goose breeding.

1. Introduction

Geese (*Anser cygnoides*) are important economic domestic poultry with a long history of domestication and abundant diversity, raised in most parts of the world [1,2]. Goose meat is an excellent animal protein source, containing all kinds of amino acids that can meet daily basic nutritional demands [3]. Goose eggs are not only a rich source of protein that is easily absorbed, but they also contain a significant amount of unsaturated fatty acids, which can aid in lowering cholesterol levels and preventing cardiovascular diseases [4]. In addition, foie gras and goose down are also of high economic value; foie gras is widely favored by diners and goose down is an excellent insulation material. Geese are raised on a huge scale in China and, as the third-largest poultry category in 2020, the total production of goose meat is up to 4.28 million tons in 2021 [5]. Until now, the breeding progress of geese has lagged behind that of chickens and ducks, primarily due to the lack of advanced breeding technologies, which hinders the overall development of the goose industry. Therefore, exploring the molecular mechanism and excavating key genes that influence goose growth is an effective method to resolve the current predicament.

Skeletal muscle is an essential organ for motion and energy metabolism, accounting for about 40% of the animal's body weight [6], and previous studies found that the weight of breast and thigh muscles account for 34% of body weight among different geese breeds [7]. Improving meat quantity and quality is an important direction in livestock. Skeletal muscle development is an elaborate process that is regulated by multi-spatial-temporal gene expression, including *MyoD*, *MyoG*, *Myf5*, and other regulatory factors [8]. Through whole-transcriptome sequencing, *LAMA4*, *SLC39A13*, *TRAF2*, *PLEKHM3*, and *PPP2R5A* were key genes to affect geese myoblast differentiation, and several circRNA-miRNA-mRNA networks synergistically regulate myogenesis in geese [9]. The liver is the largest visceral organ, which decomposes red blood cells, deposits lipids, regulates glycogen storage, and produces hormones [10]. Abundant proteins were synthesized in the liver, which are responsible for detoxification and immunity [11]. It has been reported that increased levels of antioxidative genes in goose liver is the key factor to affect body weight [12]; other studies found that hepatic glucose metabolism was necessary for geese growth [13]. Furthermore, there is a complex interaction between muscle and liver; muscle loss was found in chronic liver patients due to disturbed GH/IGF-1 axis and nitrogen homeostasis in the liver [14]. Hence, the muscular and hepatic state directly influences the animal's growth.

The Zhedong White goose is a renowned native breed in China, characterized by its rapid growth rate and raised in 19 provinces. It serves as an excellent model for exploring the mechanisms underlying goose development. In this study, we utilized transcriptomic and metabolomic analyses to identify key muscular and hepatic genes and metabolites associated with growth differences in geese. This research provides new insights into the growth of geese and identifies potential targets for molecular-assisted selection in future breeding efforts.

2. Materials and Methods

2.1. Samples

Five-hundred male Zhedong White geese were reared in a single batch under uniform conditions. Geese were housed in groups of six per cage within a closed barn, with goslings having ad libitum access to food and water. During the rearing period, the humidity was kept between 65% and 70%. For temperature control, goslings aged 1–3 weeks were initially kept at 33 °C, with the temperature decreased by 1 °C daily until reaching the outdoor temperature. Goslings aged 4–10 weeks were reared at the outdoor temperature. In terms of photoperiod management, different age groups of goslings were exposed to different durations and intensities of light: goslings aged 1–3 weeks received 24 h of light per day at an intensity of 20–30 lux/m^2, those aged 4–6 weeks were given 16–18 h of light daily at 5–10 lux/m^2, and goslings aged 7–10 weeks had 12–14 h of light daily at 5–10 lux/m^2. Their body weight (BW) was measured after a 12 h fasting period at both 1 and 70 days of age. The nutritional composition of geese is detailed in Table 1 [15]. Based on the body weight at 70 days, four healthy geese with high body weight and four with low body weight were selected for slaughter via jugular vein bleeding. The average daily gain (ADG) was calculated by subtracting the body weight at 1 day of age from the body weight at 70 days of age and dividing the result by the total number of days between these two time points. The percentage of half-eviscerated weight was determined by taking the ratio of the post-slaughter weight, after removal of the head, feet, wing tips, blood, gastrointestinal contents, and part of the viscera, to the pre-slaughter body weight. Similarly, the percentage of eviscerated weight was calculated based on the weight following the removal of the head, feet, wing tips, blood, gastrointestinal contents, all viscera, and all glands, again expressed as a percentage of the pre-slaughter body weight. For the yields of specific tissues including the head, brain, breast muscle, heart, liver, gallbladder, glandular stomach, and pancreas, they were calculated as the ratio of each respective tissue weight to the pre-slaughter body weight and expressed as a percentage. The breast muscle and liver were then isolated and quickly frozen using liquid nitrogen after weighing.

Table 1. The nutritional level of the geese diets.

Nutrition Composition	Geese Diets	
	0–28 Days	29–70 Days
Ingredients, %		
Corn grain	58.96	66.03
Soybean meal	26.67	15.81
Bran	2.30	2.10
Alfalfa meal	7.10	11.05
Soybean oil	1.85	2.00
Limestone	0.65	0.50
CaHPO$_4$	1.06	1.10
L-lysine HCl	0.11	0.21
DL-methionine	0.10	0.00
NaCl	0.20	0.20
Premix [1]	1.00	1.00
Total	100.00	100.00
Nutritional level, %		
Metabolic energy, Mcal/kg	2.90	3.00
Crude protein	19.00	15.00
Calcium	0.65	0.60
Digestibility phosphorus	0.30	0.30
Lysine	1.00	0.85
Methionine + cysteine	0.60	0.50

[1] Provided per kilogram of diet: Cu (CuSO$_4$·5H$_2$O), 8 mg; Fe (FeSO$_4$·7H$_2$O), 80 mg; Zn (ZnSO$_4$·7H$_2$O), 90 mg; Mn (MnSO$_4$·H$_2$O), 70 mg; Se (NaSeO$_3$), 0.3 mg; I (KI), 0.4 mg; Vitamin A, 9000 IU; Vitamin D3, 1600 IU; Vitamin E, 20 mg; Vitamin K3, 2 mg; Vitamin B11, 1.5 mg; Vitamin B2, 4 mg; Vitamin B6, 2 mg; niacin, 15 mg; folic acid, 0.6 mg; D-pantothenic acid, 10 mg; Vitamin B12, 0.02 mg; biotin, 0.13 mg; choline, 1000 mg.

2.2. Transcriptome Sequencing

Total RNA of muscle and liver was extracted through Trizol regent (Invitrogen, Carlsbad, CA, USA) following the manufacturer's instruction; the RNA purity and quality were measured using Nanodrop 2000 spectrophotometer (Thermo Scientific, Waltham, MA, USA) and Agilent 2100 Bioanalyzer (Agilent Technologies, Palo Alto, CA, USA). mRNA purification and library construction were based on Ribo-ZeroTM Magnetic Kit (Epicentre, Madison, WI, USA) and Hieff NGS® Ultima Dual-mode RNA Library Prep Kit (Yeasen, Shanghai, China). The paired-end sequencing method was adopted and used the Illumina Nova-Seq 6000 sequencing platform by Novogene Biotechnology Co. (Beijing, China). Acquired raw sequencing data were filtered through Fastp software (v0.21.0), and clean data were aligned with the geese reference genome (GCA_000971095.1) using Hisat2 (v2.2.1) [16]. The DESeq2 package (v1.42.0) was used to detect differentially expressed genes (DEGs) (adjusted p-value < 0.05 and $|\log2$ fold change$| > 1.0$) in muscle and liver between geese with low body weight and those with high body weight [17]. ClusterProfiler (v4.10.0) was employed to analyze the Kyoto Encyclopedia of Genes and Genomes (KEGG) pathway [18].

2.3. Metabolomic Analysis

Metabolites from the muscle and liver of Zhedong White geese were extracted by grinding the tissues with liquid nitrogen and resuspending them in prechilled 80% methanol. Equal volumes of metabolites from each sample were combined to create a quality control (QC) sample, while blank samples were prepared to remove background ions. Metabolite analysis was performed using an LC-MS/MS system in both positive and negative ion modes for relative quantification. Metabolites were identified and quantified by matching retention times and mass-to-charge ratios (m/z) against reference databases. Metabolomic data were obtained after eliminating background ions using blank samples and normalizing the data. The identified metabolites were annotated using the KEGG (https://www.genome.jp/kegg/pathway.html, accessed on 12 November 2024), HMDB (https://hmdb.ca/metabolites, accessed on 20 December 2024), and LIPIDMaps (http://www.lipidmaps.org/, accessed on 28 December 2024) databases. Metabolites with a Variable Importance in Projection (VIP) score greater than 1, a p-value less than 0.05, and a fold change of ≥ 2 or ≤ 0.5 were considered differential metabolites. The functions of these identified metabolites were further explored using the online tool MetaboAnalyst (v6.0) [19].

2.4. Quantitative Real-Time PCR

Reverse transcription of 1 μg total RNA from each sample into cDNA was performed using the PrimeScript RT Master Mix (Takara, San Jose, CA, USA) following the manufacturer's protocol. The reaction conditions were as follows: 10 min at 25 °C, 15 min at 37 °C, and 5 s at 85 °C. The resulting cDNA was stored at −20 °C. For quantitative real-time PCR (qRT-PCR) analysis on a Step-One Real-Time PCR System (Applied Biosystems, Waltham, MA, USA), a 20 μL reaction mixture was prepared containing 2 μL cDNA, 0.5 μL forward primer (10 μM), 0.5 μL reverse primer (10 μM), 10 μL 2× SYBR Premix ExTaq II (Takara), and 7 μL RNase-free H_2O. The amplification protocol consisted of an initial denaturation at 94 °C for 30 s, followed by 39 cycles of 15 s at 94 °C and 30 s at 58–62 °C. Transcript expression levels were normalized to the housekeeping gene Gapdh, and results were analyzed using the ΔΔCt method to determine fold-change relative to the control. Primer sequences are provided in Table 2.

Table 2. The primers information.

Gene	Accession No.	Primer Sequence (5′–3′)
COL11A2	XM_066986897.1	catccagctgcccaagaaga ctgcttgagggagttgaggg
COL22A1	XM_066990776.1	aggactgaggcacaaagagc cactgtatcgcaccacacct
TF	XM_013186329.3	ggaccccaaaaccaaatgcc catccagacacagcagctca
SYNC	XM_048049583.2	ggcgactacttccaggagtg gcactccttcgtcaccttga
MBOAT4	XM_013196938.3	gttgcaaagctcctctaccg tcaaggtagcacaggacagg
ANGPTL4	XM_048077583.2	cttcaggcagctacccttct atggtggtggacttcagagg
THSD4	XM_013177461.3	gctgaattgccgtgccatag ccagacacaaccttgcaagc
SOX6	XM_066997629.1	gctttccctgacatgcacaa aggtacgttttggtcgaggt
FGFRL1	XM_048048078.2	aggttccgaatccttcagca acctggctgttctttcctga
SLC25A30	XM_066988573.1	tggaatgatgcatgcactgg ctcccgaaagaatgccacac
CNST	XM_066995523.1	aaaagagacagctggggagc tcgtcatcatcatcgggctg
CREB3L3	XM_048077817.2	ccagaaccaagagctgcaga ggacctggagaaaactcgca
NR1H4	XM_048061114.2	ccatgttcctccgttcagct agcgcgtattcttcctgtgt
UAP1	XM_067001427.1	atcgggttctgcttggagaa cggtggtgaagaagtggttg
LOC106049048	XM_048054800.2	aggcttgccggtcatagttc cgggttccagttttgcagtg
PCK1	XM_013190722.3	gcagccatgagatctgaagc ttttctccatagccaggcca
GAPDH	XM_067004670.1	gagggtagtgaaggctgctg accatcaagtccaccacacg

2.5. Statistical Analysis

Data were analyzed using Prism (v.8.0; GraphPad Software, San Diego, CA, USA) for Student's *t*-test. Data were displayed as the mean ± standard deviation (SD). *p*-value < 0.05 indicated that the results were statistically significant.

3. Results

3.1. Growth Performance and Carcass Yield

A total of 500 Zhedong White geese were raised, and the top 1% of highest (HW) and lowest (LW) body weight geese at 70 days of age were collected. At 1 day of age, no significant difference in body weight was observed between the LW and HW geese. However, by day 70, body weight in the HW group was significantly greater (*p*-value < 0.05), and the average daily gain was also improved compared to the LW group (Table 3). The percentages of half-eviscerated and eviscerated weights in the HW group, along with the yields of the head, brain, breast muscle, and heart, were lower than those in the LW group. The yields of the liver, gizzard, glandular stomach, and pancreas were not changed between the two groups (*p*-value > 0.05).

Table 3. Growth performance and carcass yield of Zhedong White geese.

Item	LW	HW
BW at D1 (g)	132.25 ± 9.29	127.25 ± 1.71
BW at D70 (g)	3579.25 ± 269.53 [b]	4328.00 ± 47.83 [a]
Average daily gain (g)	49.24 ± 3.98 [b]	60.01 ± 0.68 [a]
Percentage of half-eviscerated weight (%)	75.18 ± 8.02	69.96 ± 2.35
Percentage of eviscerated weight (%)	88.63 ± 8.51	84.15 ± 2.26
Head yield (%)	4.39 ± 0.41	4.17 ± 0.16
Brain yield (‰)	2.45 ± 0.30	2.07 ± 0.14
Breast muscle yield (%)	7.48 ± 1.52	6.99 ± 0.95
Heart yield (‰)	6.90 ± 0.83	6.48 ± 0.21
Liver yield (%)	2.37 ± 0.66	3.15 ± 0.54
Gallbladder yield (‰)	1.0 ± 0.43	0.98 ± 0.34
Gizzard yield (‰)	5.25 ± 0.43	5.39 ± 0.41
Glandular stomach yield (‰)	5.04 ± 0.71	6.25 ± 2.40
Pancreas yield (%)	3.36 ± 0.14	4.01 ± 0.63

Data indicate the means of four individuals per group. [a,b]: Values within the same row with different superscripts differ significantly (p-value < 0.05).

3.2. Transcriptomic and Metabolomic Profiles of Breast Muscle

In comparison to the LW group, the HW group exhibited six up-regulated differentially expressed genes (DEGs), including COL11A2, COL22A1, and MBOAT4, and 13 downregulated DEGs, such as TF, ANGPTL4, and SYNC in breast muscle (Table S1). These DEGs were associated with the PPAR signaling pathway, adipocytokine signaling pathway, fatty acid biosynthesis, and ferroptosis (Figure 1A,B). The relative expression of selected DEGs suggested that the results from our RNA seq are accurate (Figure 1C). Additionally, a total of 59 differential metabolites were identified in the breast muscle between HW and LW geese (Table S2), related to glutathione, riboflavin, vitamin B6, and biotin metabolism (Figure 1D–F). Correlation analysis indicated that the levels of COL11A2 and COL22A1 were positively correlated with the content of S-(2-Hydroxy-3-buten-1-yl)glutathione (Figure 1G).
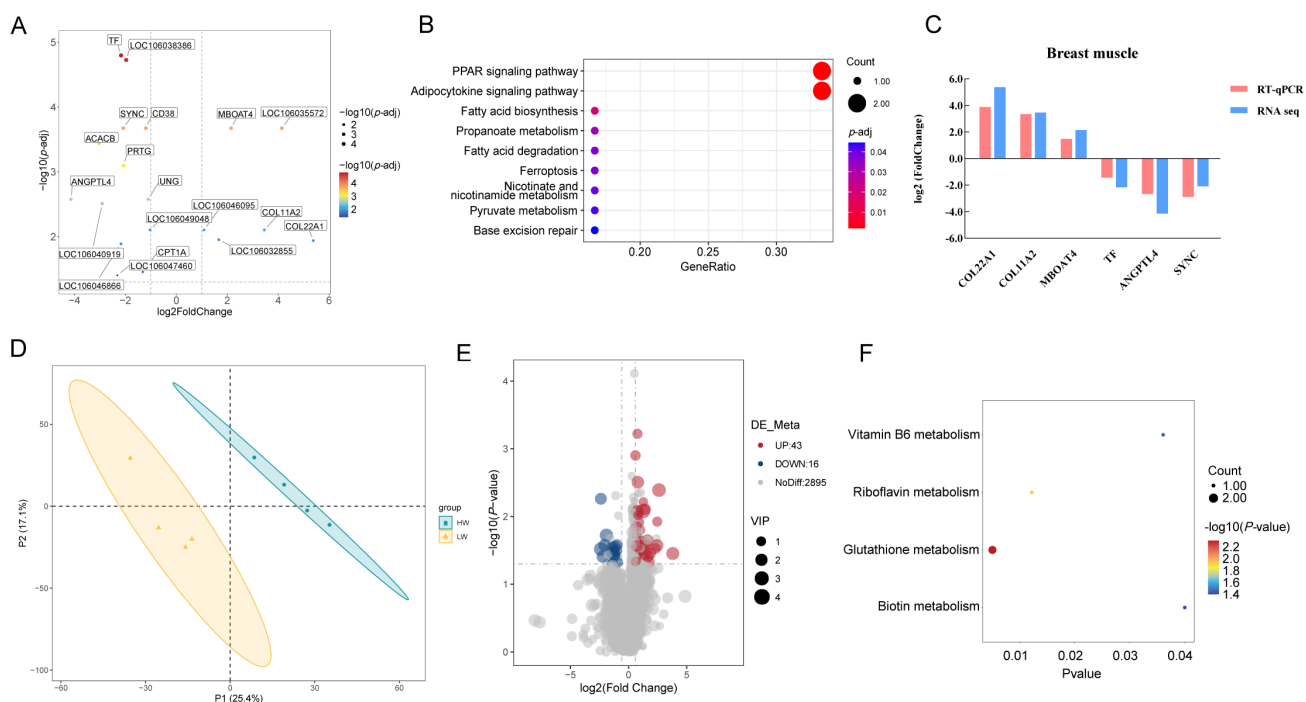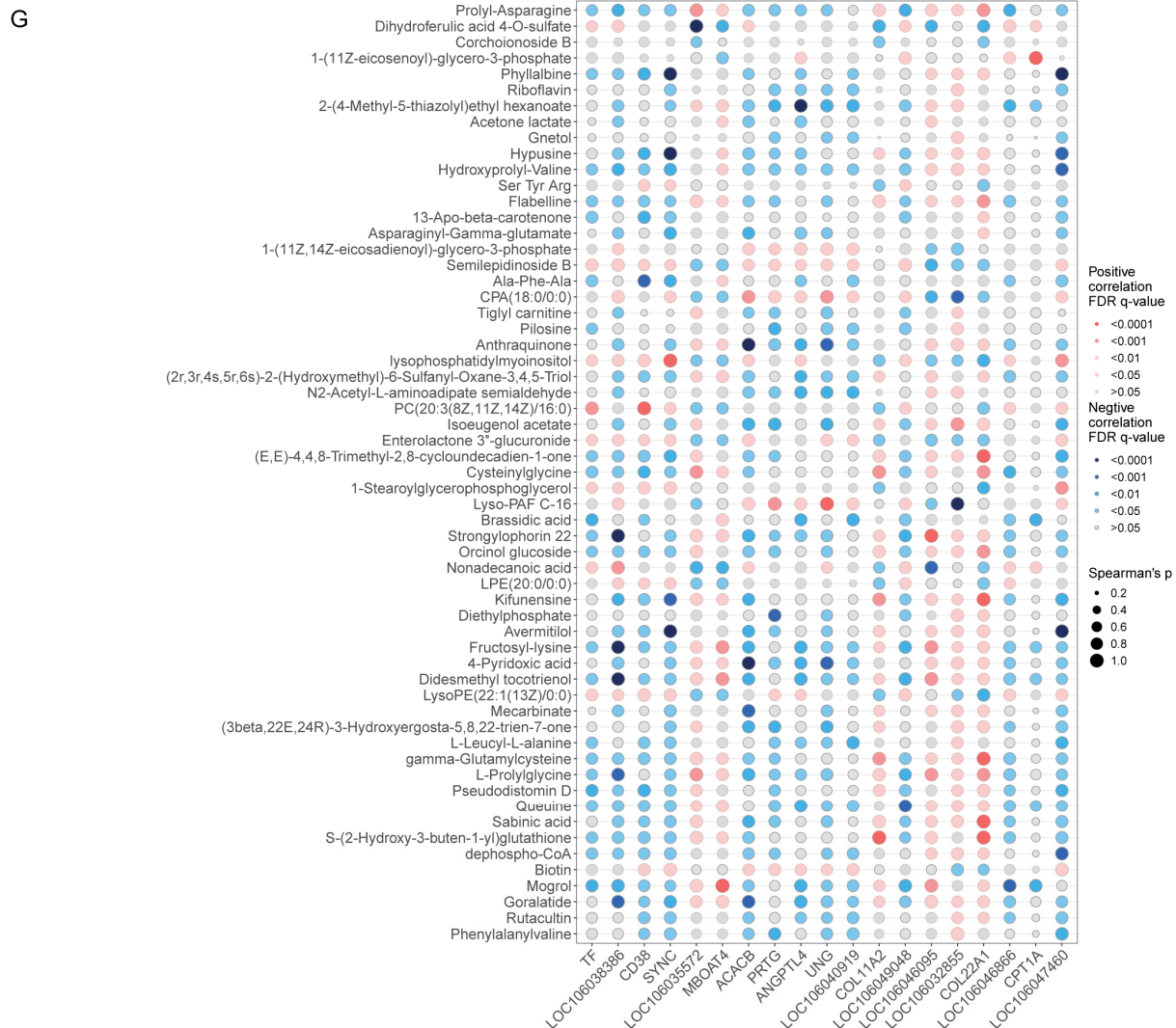

Figure 1. *Cont.*

Figure 1. Transcriptomic and metabolomic analysis of the breast muscle of Zhedong White geese with high and low body weight. (**A**) Volcano plot of DEGs in the breast muscle between the HW and LW geese. (**B**) KEGG analysis of DEGs in the breast muscle. (**C**) Validation of DEGs from breast muscle by quantitative real-time PCR. (**D**) Principal component analysis of metabolomic analysis in breast muscle. (**E**) Volcano plot of DAMs in the breast muscle of the HW and LW groups. (**F**) Functional analysis of DAMs in the breast muscle. (**G**) The conjoint analysis of DEGs and DAMs in the breast muscle.

3.3. Transcriptomic and Metabolomic Profiles of the Liver

In the liver, 43 up-regulated (i.e., THSD4, SLC25A30, SOX6, FGFRL1, and CNST) and 63 down-regulated (i.e., CREB3L3, NR1H4, LOC106049048, PCK1, and UAP1) DEGs were detected between the LW and HW groups (Table S3), which were related to the TGF-beta signaling pathway, pyruvate metabolism, glycolysis/gluconeogenesis, and the adipocytokine signaling pathway through KEGG analysis (Figure 2A,B). The protein–protein interaction network of DEGs from the liver suggested that PCK1, TFRC, and JUN may be the pivotal genes in liver to affect goose development (Figure 2C). The relative level of identified DEGs in the liver indicated that our RNA-seq is credible (Figure 2D). Through metabolome analysis, a total of 202 differential metabolites (e.g., 5,6,7,8-Tetrahydro-2,4-dimethylquinoline, 2-Hydroxyhexadecanoic acid, and coumarin) were screened between two groups (Table S4). These metabolites were involved in pyrimidine metabolism, phenylalanine, tyrosine and tryptophan biosynthesis, nitrogen metabolism, and phenylalanine

metabolism (Figure 2E,F). Conjoint analysis of the top 20 DEGs and top 30 differential metabolites showed a strongly positive correlation in THSD4 and 2-Hydroxyhexadecanoic acid with 5,6,7,8-Tetrahydro-2,4-dimethylquinoline (Figure 2G).
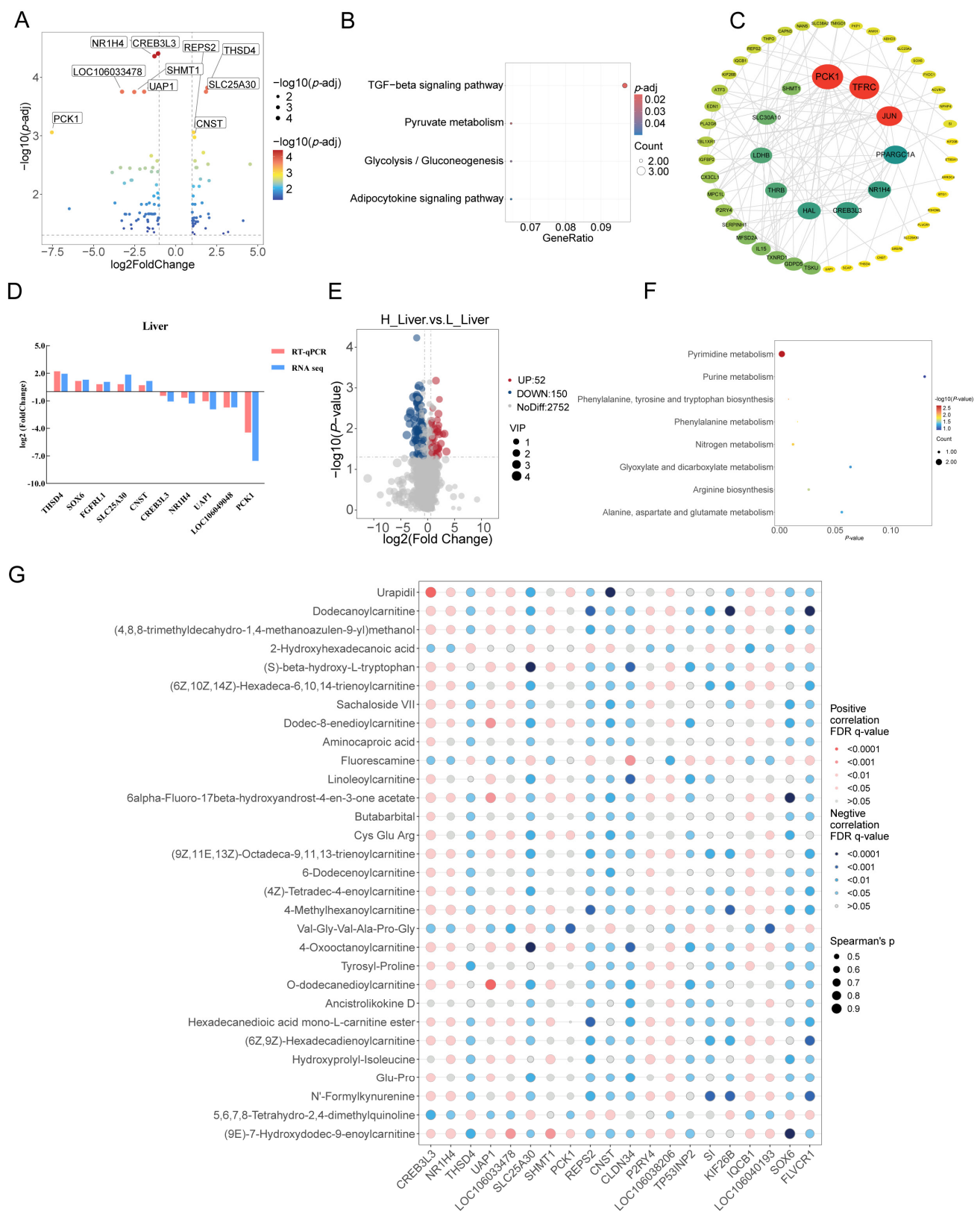

Figure 2. Transcriptomic and metabolomic analysis of the liver of Zhedong White geese of the HW and LW groups. (**A**) Volcano plot of DEGs in the liver of the HW and LW geese. (**B**) KEGG analysis

of DEGs from the liver. (**C**) The protein–protein interaction network from hepatic DEGs between the two groups. (**D**) Validation of DEGs from liver by quantitative real-time PCR. (**E**) Volcano plot of DAMs in the liver of the HW and LW geese. (**F**) Functional analysis of DAMs in the liver. (**G**) The conjoint analysis of DEGs and DAMs in the liver.

3.4. The Interplay Between the Breast Muscle and Liver

To investigate potential liver–muscle crosstalk, we identified shared DEGs and DAMs between the liver and breast muscle. One DEG, LOC106049048, was down-regulated in both the liver and muscle of the HW group. Additionally, four DAMs—mogrol, brassidic acid, flabelline, and L-Leucyl-L-alanine—were found in both tissues (Figure 3). Notably, the relative contents of mogrol, brassidic acid, and flabelline were consistently increased between the muscle and liver in the HW group (*p*-value < 0.05).
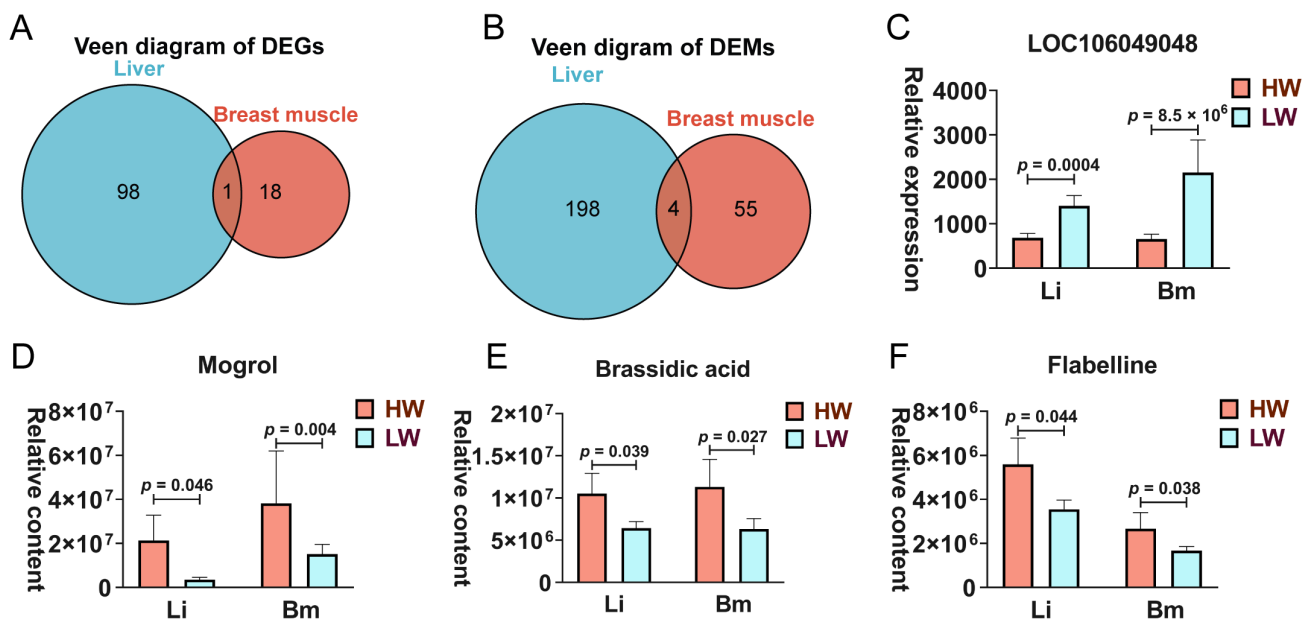
Figure 3. The conjoint analysis of DEGs and DAMs in the breast muscle and liver. (**A**) The Venn diagram of DEGs from the breast muscle and liver. (**B**) The Venn diagram of DAMs from the breast muscle and liver. (**C**) The level of LOC106049048 in the breast muscle and liver. The content of mogrol (**D**), brassidic acid (**E**), and flabelline (**F**). Li: liver; Bm: breast muscle.

4. Discussion

As consumer living conditions improve, geese have gained popularity for their meat, eggs, foie gras, and down, with better growth performance yielding increased economic benefits. However, the mechanisms underlying goose growth remain poorly understood. In this study, 500 Zhedong White geese were raised, and eight geese (four high-weight and four low-weight) were selected based on their body weight at 70 days. The body weight of the high-weight group was, on average, 748.75 g heavier than that of the low-weight group, and the average daily gain of the high-weight geese exceeded that of the low-weight geese by 10.77 g (*p*-value < 0.05). The yields of digestive organs (liver, gizzard, glandular stomach, and pancreas) displayed no significant difference between the LW and HW groups; the percentage of half-eviscerated weight and eviscerated weight was also shown to be stable between two groups, which may have resulted from the limited samples employed in this study. A previous study indicated that geese with higher feeding intake rates exhibited increased body weight and liver weight [20]. Thus, the enhanced yield of digestive organs in the high-weight geese may contribute to the improved digestion and absorption of nutrients, ultimately accelerating their growth rate.

Skeletal muscle is a vital organ for motion and metabolism, comprising approximately 40% of body weight. While the yield of breast muscle showed no significant difference between the HW and LW groups, the weight of breast muscle in the HW geese was indeed higher than that in the LW geese (*p*-value < 0.05). To explore the changes in breast muscle, transcriptomic and metabolomic analyses were performed to detect key genes and metabolites. In breast muscle, 19 differentially expressed genes were detected between the two groups, including *COL22A1*, *COL11A2*, and *ANGPTL4*. *COL22A1* encodes the synthesis of collagen XXII; the knockout of *COL22A1* in zebrafish resulted in a muscular dystrophy-like phenotype and exogenous COLXXII could rescue the defect [21]. Recent single-cell RNA-sequencing of skeletal muscle indicated that *COL22A1* located at the end of myofiber may influence muscle development by regulating the function of the neuromuscular junction [22,23]. *COL11A2* (collagen type XI alpha 2 chain) is pivotal for vertebral development, and was determined as a candidate gene for the body length of pigs [24], large yellow croakers [25], mice [26], and goats [27]. *ANGPTL4* is an angiopoietin-like protein that regulates fat metabolism; previous studies found that the body weight and fecal fat content were higher in *ANGPTL4*-deficient mice than in wild-type mice [28] and increased levels of *ANGPTL4* induced by linoleic acid inhibit myoblast differentiation through suppressing Wnt/β-catenin signaling pathway [29]. Through metabolomic analysis, the contents of 59 metabolites were significantly different in breast muscle between the HW and LW geese, and were involved in glutathione metabolism, vitamin B6 metabolism, riboflavin metabolism, and biotin metabolism. Conjoint analysis of DEGs and DAMs showed a strong positive correlation between S-(2-Hydroxy-3-buten-1-yl)glutathione and both *COL11A2* and *COL22A1*; the results indicated that *COL11A2* with *COL22A1* may influence skeletal muscle development by regulating glutathione metabolism.

In this study, a total of 99 DEGs (i.e., *THSD4*, *CREB3L3*, and *NR1H4*) of the liver were identified between HW and LW groups, and they were involved in the signaling pathway of cytokine–cytokine receptor interaction, pyruvate metabolism, glycolysis, and several regulations of the development process. *THSD4* (Thrombospondin Type 1 Domain Containing 4) is a protein-coding gene with a hydrolase activity that was identified as a candidate gene for body fatness in mice [30]. Previous suggested patients with THSD4 mutation showed skeletal defects [31], and the gene has also been identified as a candidate gene that influenced broilers' growth and meat quality [32]. *CREB3L3* (cAMP-responsive element-binding protein 3-like 3) is a membrane-bound transcription factor that could be activated during fasting to regulate triglyceride metabolism, it has been reported that the increase in body weight from the *CREB3L3*-overexpressed mouse was significantly inhibited during high-fat and high-sucrose feeding [33]. Another study proved that the level of plasma triglycerides in CREB3L3 knockout mice was increased, and the deficiency in CREB3L3 activated the hepatic-proliferative function [34]. *NR1H4* could function as a receptor for hepatic bile acid, and its mutation changed the level of fasting glucose and free fatty acid [35]; other studies proved that *NR1H4* was a key regulated gene related to liver development and an upregulated level of *NR1H4* would inhibit lipid synthesis [36]. Through metabolomic analysis, 202 differential metabolites were detected in the liver between the HW and LW geese, and these were involved in pyrimidine metabolism, nitrogen metabolism, phenylalanine metabolism, arginine biosynthesis, and phenylalanine, tyrosine and tryptophan biosynthesis. Various amino acid biosynthesis in the liver is essential for animal growth. Through conjoint analysis of DEGs and DAMs, the level of *THSD4* was positively correlated with the content of 2-Hydroxyhexadecanoic acid. Former studies compared the differential metabolites between sheep with high body weight and those with low body weight and found that the content of 2-Hydroxyhexadecanoic acid was increased in the muscle and rumen content of sheep with high body weight [37,38].

LOC106049048 (*ACAD11L*) is an acyl-CoA dehydrogenase family member 11-like protein, the shared DEG in the liver and the breast muscle. *ACAD11* and *ACAD10* regulate mammalian 4-hydroxy acid lipid catabolism, and previous studies found that the knockout of *ACAD11* slightly increased the body weight of mice [39], *ACAD10*-deficient mice showed enhanced mass of liver, epididymal fat, and tibialis anterior muscle [40]. Therefore, the down-regulated expression of *LOC106049048* may promote the geese's growth by regulating the lipid metabolism of the geese's skeletal muscle and liver. Compared with the LW group, the contents of mogrol, brassidic acid, and flabelline were increased in liver and breast muscle in the HW group. Mogrol is a pharmacologically active ingredient isolated from the fruits of *Siraitia grosvenorii* that could relieve the development of pulmonary fibrosis and hyperglycemia [41,42]. The trans-isomer of erucic acid is brassidic acid, which is a bioactive substance that has antimicrobial action [43]. Based on these findings, we hypothesized that geese's growth was potentially influenced by altering the metabolism of breast muscle and liver.

5. Conclusions

In this study, we systematically identified the differential genes and metabolites in the liver and breast muscles of geese with varying growth performances. Our findings enhance the understanding of the transcriptomic and metabolomic basis underlying high and low growth performance in Zhedong White geese. The potential genes and metabolites identified can serve as selection markers in breeding programs aimed at promoting growth performance, although further functional validation is necessary in subsequent studies.

Conflicts of Interest: The authors declare no conflicts of interest.

References

1. Shi, X.-W.; Wang, J.-W.; Zeng, F.-T.; Qiu, X.-P. Mitochondrial DNA Cleavage Patterns Distinguish Independent Origin of Chinese Domestic Geese and Western Domestic Geese. *Biochem. Genet.* **2006**, *44*, 237–245. [CrossRef]

2. Heikkinen, M.E.; Ruokonen, M.; Alexander, M.; Aspi, J.; Pyhäjärvi, T.; Searle, J.B. Relationship between Wild Greylag and European Domestic Geese Based on Mitochondrial DNA. *Anim. Genet.* **2015**, *46*, 485–497. [CrossRef] [PubMed]

3. Haraf, G.; Wołoszyn, J.; Okruszek, A.; Goluch, Z.; Wereńska, M.; Teleszko, M. The Protein and Fat Quality of Thigh Muscles from Polish Goose Varieties. *Poult. Sci.* **2021**, *100*, 100992. [CrossRef]

4. Krittanawong, C.; Narasimhan, B.; Wang, Z.; Virk, H.U.H.; Farrell, A.M.; Zhang, H.; Tang, W.H.W. Association Between Egg Consumption and Risk of Cardiovascular Outcomes: A Systematic Review and Meta-Analysis. *Am. J. Med.* **2021**, *134*, 76–83.e2. [CrossRef]

5. Zhang, Y.; Qi, S.; Fan, S.; Jin, Z.; Bao, Q.; Zhang, Y.; Zhang, Y.; Xu, Q.; Chen, G. Comparison of Growth Performance, Meat Quality, and Blood Biochemical Indexes of Yangzhou Goose under Different Feeding Patterns. *Poult. Sci.* **2024**, *103*, 103349. [CrossRef] [PubMed]

6. Güller, I.; Russell, A.P. MicroRNAs in Skeletal Muscle: Their Role and Regulation in Development, Disease and Function. *J. Physiol.* **2010**, *588*, 4075–4087. [CrossRef] [PubMed]

7. Boz, M.A.; Oz, F.; Yamak, U.S.; Sarica, M.; Cilavdaroglu, E. The Carcass Traits, Carcass Nutrient Composition, Amino Acid, Fatty Acid, and Cholesterol Contents of Local Turkish Goose Varieties Reared in an Extensive Production System. *Poult. Sci.* **2019**, *98*, 3067–3080. [CrossRef]

8. Shi, K.; Lu, Y.; Chen, X.; Li, D.; Du, W.; Yu, M. Effects of Ten-Eleven Translocation-2 (Tet2) on Myogenic Differentiation of Chicken Myoblasts. *Comp. Biochem. Physiol. B Biochem. Mol. Biol.* **2021**, *252*, 110540. [CrossRef]

9. Xiao, L.; Chen, J.; He, X.; Zhang, X.; Luo, W. Whole-Transcriptome Sequencing Revealed the ceRNA Regulatory Network during the Proliferation and Differentiation of Goose Myoblast. *Poult. Sci.* **2024**, *103*, 104173. [CrossRef]

10. Brockmöller, J.; Roots, I. Assessment of Liver Metabolic Function. Clinical Implications. *Clin. Pharmacokinet.* **1994**, *27*, 216–248. [CrossRef]

11. Chen, R.; Jiang, X.; Sun, D.; Han, G.; Wang, F.; Ye, M.; Wang, L.; Zou, H. Glycoproteomics Analysis of Human Liver Tissue by Combination of Multiple Enzyme Digestion and Hydrazide Chemistry. *J. Proteome Res.* **2009**, *8*, 651–661. [CrossRef] [PubMed]

12. Ren, Y.; Sun, Y.; Javad, H.U.; Wang, R.; Zhou, Z.; Huang, Y.; Shu, X.; Li, C. Growth Performance of and Liver Function in Heat-Stressed Magang Geese Fed the Antioxidant Zinc Ascorbate and Its Potential Mechanism of Action. *Biol. Trace Elem. Res.* **2024**, *203*, 1035–1047. [CrossRef] [PubMed]

13. Xu, C.; Yang, Z.; Yang, Z.F.; He, X.X.; Zhang, C.Y.; Yang, H.M.; Rose, S.P.; Wang, Z.Y. Effects of Different Dietary Starch Sources on Growth and Glucose Metabolism of Geese. *Poult. Sci.* **2023**, *102*, 102362. [CrossRef] [PubMed]

14. De Bandt, J.-P.; Jegatheesan, P.; Tennoune-El-Hafaia, N. Muscle Loss in Chronic Liver Diseases: The Example of Nonalcoholic Liver Disease. *Nutrients* **2018**, *10*, 1195. [CrossRef]

15. Zhu, X.; Shao, B.; Guo, Y.; Gao, L.; Zhang, H.; Chen, W.; Wang, Y.; Gao, G.; Huang, Y. Incidence Rate of Angel Wing and Its Effect on Wing Bone Development and Serum Biochemical Parameters in Geese. *Poult. Sci.* **2021**, *100*, 101450. [CrossRef]

16. Kim, D.; Paggi, J.M.; Park, C.; Bennett, C.; Salzberg, S.L. Graph-Based Genome Alignment and Genotyping with HISAT2 and HISAT-Genotype. *Nat. Biotechnol.* **2019**, *37*, 907–915. [CrossRef]

17. Love, M.I.; Huber, W.; Anders, S. Moderated Estimation of Fold Change and Dispersion for RNA-Seq Data with DESeq2. *Genome Biol.* **2014**, *15*, 550. [CrossRef]

18. Yu, G.; Wang, L.-G.; Han, Y.; He, Q.-Y. clusterProfiler: An R Package for Comparing Biological Themes among Gene Clusters. *OMICS* **2012**, *16*, 284–287. [CrossRef]

19. Pang, Z.; Lu, Y.; Zhou, G.; Hui, F.; Xu, L.; Viau, C.; Spigelman, A.F.; MacDonald, P.E.; Wishart, D.S.; Li, S.; et al. MetaboAnalyst 6.0: Towards a Unified Platform for Metabolomics Data Processing, Analysis and Interpretation. *Nucleic Acids Res.* **2024**, *52*, W398–W406. [CrossRef]

20. Kong, J.; Yao, Z.; Chen, J.; Zhao, Q.; Li, T.; Dong, M.; Bai, Y.; Liu, Y.; Lin, Z.; Xie, Q.; et al. Comparative Transcriptome Analysis Unveils Regulatory Factors Influencing Fatty Liver Development in Lion-Head Geese under High-Intake Feeding Compared to Normal Feeding. *Vet. Sci.* **2024**, *11*, 366. [CrossRef]

21. Charvet, B.; Guiraud, A.; Malbouyres, M.; Zwolanek, D.; Guillon, E.; Bretaud, S.; Monnot, C.; Schulze, J.; Bader, H.L.; Allard, B.; et al. Knockdown of Col22a1 Gene in Zebrafish Induces a Muscular Dystrophy by Disruption of the Myotendinous Junction. *Development* **2013**, *140*, 4602–4613. [CrossRef]

22. Petrany, M.J.; Swoboda, C.O.; Sun, C.; Chetal, K.; Chen, X.; Weirauch, M.T.; Salomonis, N.; Millay, D.P. Single-Nucleus RNA-Seq Identifies Transcriptional Heterogeneity in Multinucleated Skeletal Myofibers. *Nat. Commun.* **2020**, *11*, 6374. [CrossRef]

23. Kim, M.; Franke, V.; Brandt, B.; Lowenstein, E.D.; Schöwel, V.; Spuler, S.; Akalin, A.; Birchmeier, C. Single-Nucleus Transcriptomics Reveals Functional Compartmentalization in Syncytial Skeletal Muscle Cells. *Nat. Commun.* **2020**, *11*, 6375. [CrossRef]

24. Wang, H.; Wang, X.; Li, M.; Sun, H.; Chen, Q.; Yan, D.; Dong, X.; Pan, Y.; Lu, S. Genome-Wide Association Study of Growth Traits in a Four-Way Crossbred Pig Population. *Genes* **2022**, *13*, 1990. [CrossRef] [PubMed]

25. Zhou, Z.; Han, K.; Wu, Y.; Bai, H.; Ke, Q.; Pu, F.; Wang, Y.; Xu, P. Genome-Wide Association Study of Growth and Body-Shape-Related Traits in Large Yellow Croaker (*Larimichthys crocea*) Using ddRAD Sequencing. *Mar. Biotechnol.* **2019**, *21*, 655–670. [CrossRef] [PubMed]

26. Eppig, J.T.; Bult, C.J.; Kadin, J.A.; Richardson, J.E.; Blake, J.A. The Mouse Genome Database (MGD): From Genes to Mice—A Community Resource for Mouse Biology. *Nucleic Acids Res.* **2005**, *33*, D471–D475. [CrossRef] [PubMed]

27. Gao, J.; Lyu, Y.; Zhang, D.; Reddi, K.K.; Sun, F.; Yi, J.; Liu, C.; Li, H.; Yao, H.; Dai, J.; et al. Genomic Characteristics and Selection Signatures in Indigenous Chongming White Goat (*Capra hircus*). *Front. Genet.* **2020**, *11*, 901. [CrossRef]

28. Mattijssen, F.; Alex, S.; Swarts, H.J.; Groen, A.K.; van Schothorst, E.M.; Kersten, S. Angptl4 Serves as an Endogenous Inhibitor of Intestinal Lipid Digestion. *Mol. Metab.* **2014**, *3*, 135–144. [CrossRef]

29. Son, Y.; Lorenz, W.W.; Paton, C.M. Linoleic Acid-Induced ANGPTL4 Inhibits C2C12 Skeletal Muscle Differentiation by Suppressing Wnt/β-Catenin. *J. Nutr. Biochem.* **2023**, *116*, 109324. [CrossRef]

30. McDaniel, A.H.; Li, X.; Tordoff, M.G.; Bachmanov, A.A.; Reed, D.R. A Locus on Mouse Chromosome 9 (Adip5) Affects the Relative Weight of the Gonadal but Not Retroperitoneal Adipose Depot. *Mamm. Genome* **2006**, *17*, 1078–1092. [CrossRef]

31. Elbitar, S.; Renard, M.; Arnaud, P.; Hanna, N.; Jacob, M.-P.; Guo, D.-C.; Tsutsui, K.; Gross, M.-S.; Kessler, K.; Tosolini, L.; et al. Pathogenic Variants in THSD4, Encoding the ADAMTS-like 6 Protein, Predispose to Inherited Thoracic Aortic Aneurysm. *Genet. Med.* **2021**, *23*, 111–122. [CrossRef] [PubMed]

32. Seifi Moroudi, R.; Ansari Mahyari, S.; Vaez Torshizi, R.; Lanjanian, H.; Masoudi-Nejad, A. Identification of New Genes and Quantitative Trait Locis Associated with Growth Curve Parameters in F2 Chicken Population Using Genome-Wide Association Study. *Anim. Genet.* **2021**, *52*, 171–184. [CrossRef]

33. Nakagawa, Y.; Satoh, A.; Yabe, S.; Furusawa, M.; Tokushige, N.; Tezuka, H.; Mikami, M.; Iwata, W.; Shingyouchi, A.; Matsuzaka, T.; et al. Hepatic CREB3L3 Controls Whole-Body Energy Homeostasis and Improves Obesity and Diabetes. *Endocrinology* **2014**, *155*, 4706–4719. [CrossRef]

34. Ruppert, P.M.M.; Park, J.-G.; Xu, X.; Hur, K.Y.; Lee, A.-H.; Kersten, S. Transcriptional Profiling of PPARα$^{-/-}$ and CREB3L3$^{-/-}$ Livers Reveals Disparate Regulation of Hepatoproliferative and Metabolic Functions of PPARα. *BMC Genom.* **2019**, *20*, 199. [CrossRef] [PubMed]

35. Heni, M.; Wagner, R.; Ketterer, C.; Böhm, A.; Linder, K.; Machicao, F.; Machann, J.; Schick, F.; Hennige, A.M.; Stefan, N.; et al. Genetic Variation in NR1H4 Encoding the Bile Acid Receptor FXR Determines Fasting Glucose and Free Fatty Acid Levels in Humans. *J. Clin. Endocrinol. Metab.* **2013**, *98*, E1224–E1229. [CrossRef]

36. Cogburn, L.A.; Trakooljul, N.; Chen, C.; Huang, H.; Wu, C.H.; Carré, W.; Wang, X.; White, H.B. Transcriptional Profiling of Liver during the Critical Embryo-to-Hatchling Transition Period in the Chicken (*Gallus gallus*). *BMC Genom.* **2018**, *19*, 695. [CrossRef]

37. Li, H.; Yu, Q.; Li, T.; Shao, L.; Su, M.; Zhou, H.; Qu, J. Rumen Microbiome and Metabolome of Tibetan Sheep (Ovis Aries) Reflect Animal Age and Nutritional Requirement. *Front. Vet. Sci.* **2020**, *7*, 609. [CrossRef] [PubMed]

38. Zhang, X.Y.; Yuan, Z.H.; Li, F.D.; Yue, X.P. Integrating Transcriptome and Metabolome to Identify Key Genes Regulating Important Muscular Flavour Precursors in Sheep. *Animal* **2022**, *16*, 100679. [CrossRef]

39. Rashan, E.H.; Bartlett, A.K.; Khana, D.B.; Zhang, J.; Jain, R.; Smith, A.J.; Baker, Z.N.; Cook, T.; Caldwell, A.; Chevalier, A.R.; et al. ACAD10 and ACAD11 Enable Mammalian 4-Hydroxy Acid Lipid Catabolism. *bioRxiv* **2024**, 2024.01.09.574893. [CrossRef]

40. Yew, M.J.; Heywood, S.E.; Ng, J.; West, O.M.; Pal, M.; Kueh, A.; Lancaster, G.I.; Myers, S.; Yang, C.; Liu, Y.; et al. ACAD10 Is Not Required for Metformin's Metabolic Actions or for Maintenance of Whole-body Metabolism in C57BL/6J Mice. *Diabetes Obes. Metab.* **2024**, *26*, 1731–1745. [CrossRef]

41. Liu, B.; Yang, J.; Hao, J.; Xie, H.; Shimizu, K.; Li, R.; Zhang, C. Natural Product Mogrol Attenuates Bleomycin-Induced Pulmonary Fibrosis Development through Promoting AMPK Activation. *J. Funct. Foods* **2021**, *77*, 104280. [CrossRef]

42. Tanaka, C.; Harada, N.; Teraoka, Y.; Urushizaki, H.; Shinmori, Y.; Onishi, T.; Yotsumoto, Y.; Ito, Y.; Kitakaze, T.; Inui, T.; et al. Mogrol Stimulates G-Protein-Coupled Bile Acid Receptor 1 (GPBAR1/TGR5) and Insulin Secretion from Pancreatic β-Cells and Alleviates Hyperglycemia in Mice. *Sci. Rep.* **2024**, *14*, 3244. [CrossRef] [PubMed]

43. Kim, S.-J.; Jin, S.; Ishii, G. Isolation and Structural Elucidation of 4-(Beta-D-Glucopyranosyldisulfanyl)Butyl Glucosinolate from Leaves of Rocket Salad (*Eruca sativa* L.) and Its Antioxidative Activity. *Biosci. Biotechnol. Biochem.* **2004**, *68*, 2444–2450. [CrossRef] [PubMed]